

Mechanical response of NiFeGa alloys containing second-phase particles

R.F. Hamilton,^a H. Sehitoglu,^{a,*} C. Efstathiou^a and H.J. Maier^b

^aUniversity of Illinois, Department of Mechanical Science and Engineering, 1206 W. Green Street, Urbana, IL 61801, USA

^bUniversity of Paderborn, Lehrstuhl f. Werkstoffkunde, D-33095 Paderborn, Germany

Received 17 April 2007; revised 15 May 2007; accepted 21 May 2007

Available online 20 June 2007

Tensile and compressive strain–temperature and stress–strain responses have been used for the first time to investigate the effects of second-phase particles on the deformation of NiFeGa shape memory alloys. Particles are conducive to the dissipation of stored energy; stress and thermal hysteresis increase three-fold in aged alloys. Although dissipation is severe, recoverable strain levels are as large as +12% and –6%, which match strains for the unaged alloys. These results demonstrate that second-phase particles can be used to tailor the hysteresis while maintaining large transformation strains.

© 2007 Published by Elsevier Ltd. on behalf of Acta Materialia Inc.

Keywords: Shape memory; Annealing; Microstructure; Stress–strain asymmetry; Strain–temperature asymmetry

Shape memory alloys (SMAs) undergo a martensitic transformation (MT) under applied load or temperature change resulting in a transformation of the crystal structure from an austenite parent phase to a martensite product phase. Deformation is completely recoverable, albeit with hysteresis, with strain levels depending on the composition of the austenite matrix and the crystal structures of the austenite and martensite phases. Precipitation of second-phases into the matrix of shape memory materials alters the MT by changing the austenite composition and/or altering martensite nucleation and growth [1]. Consequently, creating a dual-phase matrix allows the pseudoelastic and shape memory response to be tailored. For example, internal stress fields near Ti_3Ni_4 precipitates in Nitinol alloys can facilitate nucleation, and thus modify transformation temperatures and stresses [1–3].

Ferromagnetic shape memory alloys (FSMAs) are classes of SMAs in which the application of an external magnetic field causes a MT in the ferromagnetic state. NiFeGa FSMAs exhibit outstanding stress–strain ($\sigma - \varepsilon$) and strain–temperature ($\varepsilon - T$) responses, which, without heat treatment, completely recover +12% and –6% strain, while exhibiting some of the smallest thermal ($\sim 2^\circ\text{C}$) and stress ($< 30\text{ MPa}$) hysteresis observed

to date [4–7]. For NiFeGa alloys, holding temperatures of $\sim 1000^\circ\text{C}$ enable precipitation of second-phase (γ -phase) particles with a face-centered cubic (fcc) A1 structure [8–10]. The current literature does not consider how γ -phase particles affect $\sigma - \varepsilon$ and $\varepsilon - T$ responses, which are benchmarks when characterizing precipitated SMAs for applications such as SMA actuators.

The present paper demonstrates the asymmetric $\sigma - \varepsilon$ responses of two-phase ($\gamma +$ austenite) NiFeGa alloys. Tensile and compressive $\varepsilon - T$ responses are studied for the first time. To circumvent grain boundary effects, single crystalline materials are investigated. The results of this comprehensive experimental program underscore that incorporating the γ -phase into the microstructure allows the hysteresis to be tailored while preserving the large recoverable strains observed in unaged NiFeGa alloys.

Single crystalline $\text{Ni}_{54}\text{Fe}_{19}\text{Ga}_{27}$ alloys of [001] orientation were heat treated at 900°C for 3 h following single crystal growth and subsequently water quenched. Details of the crystal growth process and heat treatment are included in our previous work [6]. The optical micrograph in Figure 1, taken at room temperature, shows the γ -phase. For the isothermal $\sigma - \varepsilon$ response, the applied strain was incremented from $\pm 2\%$ up to +12% and –6% to ascertain the influence of particles on partial and complete hysteresis loops. For the $\varepsilon - T$ responses, the compressive and tensile iso-stresses (i.e. constant stress) were monotonically increased from $\pm 10\text{ MPa}$ to

* Corresponding author. Tel.: +1 217 3334112; fax: +1 217 2446534; e-mail: huseyin@uiuc.edu

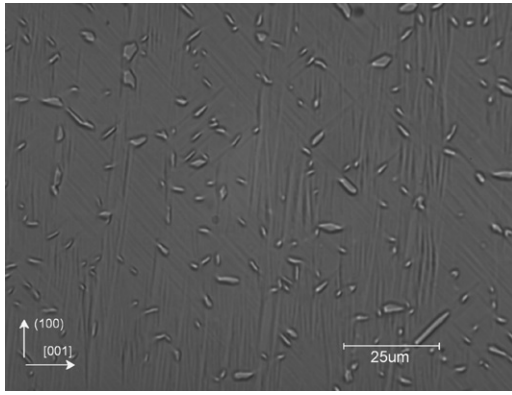


Figure 1. Optical micrograph at $T = 25\text{ }^\circ\text{C}$ showing a fine distribution of γ -phase particles and martensite platelets.

ascertain the influences of γ -phase particles at very low stress levels.

Representative tensile and compressive $\sigma - \epsilon$ responses of aged [001] oriented $\text{Ni}_{54}\text{Fe}_{19}\text{Ga}_{27}$ alloys are included in Figure 2. The temperature of $T = 75\text{ }^\circ\text{C}$ exceeds A_f by about $40\text{ }^\circ\text{C}$, and thus the austenite is stable, ensuring that recovery is pseudoelastic. Transformation stresses exhibit stark asymmetry. Note the slight drop in tensile transformation stress at the maximum applied strain, whereas the compressive stress is stable. The stress hysteresis $\Delta\sigma_m$ is defined at half the applied strain in the figure. When the maximum recoverable strain is reached in each strain direction, the complete hysteresis loops exhibit comparable magnitudes. The dependence of $\Delta\sigma_m$ on the applied strain for the aged and unaged alloys is shown in the inset figure. Aging produces nearly 50 MPa wider $\Delta\sigma_m$ for partial and complete hysteresis loops in tension and compression.

Tensile and compressive $\epsilon - T$ responses for the aged and unaged states are included in Figure 3. At $+40$ and -100 MPa , the heating and cooling segments extraordinarily intersect for the unaged state, whereas they are separated after aging. As a result, the temperature hysteresis ΔT_m measured is markedly wider for the aged alloy and widens most significantly in tension. The inset figure illustrates that, in each stress state, the maximum recoverable strains are identical for the unaged and aged states. To demonstrate the effects of precipitation on the

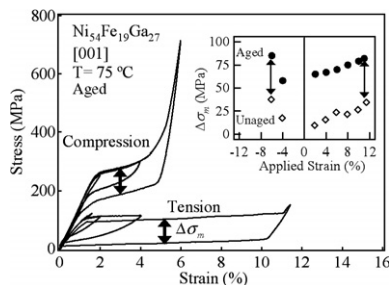


Figure 2. Tensile and compressive stress–strain responses at $T = 75\text{ }^\circ\text{C}$. At the maximum applied strain, the compressive and tensile stress hysteresis $\Delta\sigma_m$ are identical. In the inset figure, arrows highlight that the difference between $\Delta\sigma_m$ in unaged and aged alloys is equivalent for each strain direction.

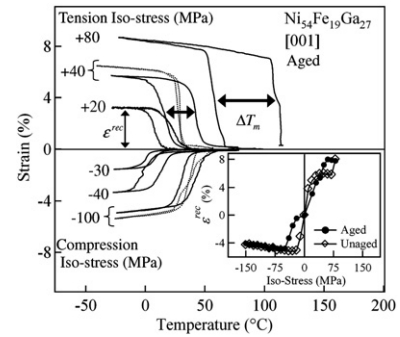


Figure 3. Tensile and compressive strain–temperature responses at increasing iso-stress levels. Aging facilitates a strikingly wider temperature hysteresis ΔT_m (horizontal double arrow), shown at $+40$ and -100 MPa , which exhibits intersecting heating and cooling segments in the unaged state (dotted line). In the inset figure, each stress state attains maximum recoverable strains ϵ^{rec} (vertical double arrow) that are equal for unaged and aged alloys.

transformation temperatures, the forward and reverse transformation start temperatures, M_s and A_s , respectively, are plotted as a function of iso-stress in Figure 4. As expected, the temperatures increase with increasing compressive or tensile iso-stress. The aged and unaged alloys exhibit similar transformation temperatures in compression; however, in tension, the temperatures become strikingly higher for the aged alloy when the iso-stress exceeds $+50\text{ MPa}$.

Ultimately, the outstanding consequence of the γ -phase particles resulting from aging is wider hysteresis levels (Figs. 2 and 3). Hysteresis growth is attributed to irreversible/dissipative mechanisms associated with the inclusion of γ -phase particles in the microstructure. As the transformation front bypasses the particles, frictional work is expended, and thus dissipation is enhanced. Energy-dispersive X-ray (EDX) analysis shows that the composition of the γ -phase is $\text{Ni}_{54.3}\text{Ga}_{18.3}\text{Fe}_{27.4}$ (at.%). Based on the Fe content, the phase should not undergo a martensitic transformation, and thus plastic accommodation can occur at the interface between the second-phase and the matrix as observed in a similar class of alloys, CoNiAl [11]. Plasticity which develops in this manner is irreversible; hence, it promotes hysteresis growth.

In tension, the much larger temperature hysteresis is attributed to significant dislocation generation. Tensile

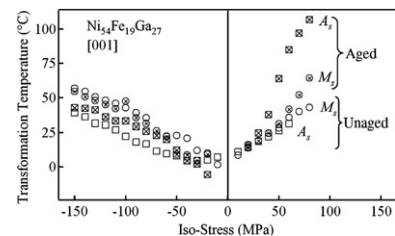


Figure 4. The forward (M_s) and reverse (A_s) transformation start temperatures as a function of iso-stress for the aged (filled markers) and unaged (open markers) states. In the aged state, the transformation temperatures increase drastically in tension with increasing iso-stress.

transformation strains exhibit incomplete recovery in tension at +80 MPa in Figure 3, which demonstrates that plasticity prevails. Dislocation generation, and thus plasticity, is less significant in compression and complete recovery is observed up to –100 MPa. Dislocations and residual martensite from prior thermal cycles become catalysts for nucleation in subsequent transformations, enabling higher M_s temperatures. Since the M_s temperatures in tension increase greatly after aging and the temperatures are comparable in compression (Fig. 4), dislocations and residual martensite are most substantial in tension. The slight drop in transformation stress in Figure 2 is analogous to increasing M_s , and thus is attributed to similar mechanisms. Indeed, transmission electron microscopy (TEM) reveals dense dislocation arrays after thermal cycling in tension (Fig. 5a). The linear features in Figure 5b are likely dislocations, which can facilitate the tweed contrasts in the figure, which is a well-known pre-martensitic phenomenon. The streaks in the corresponding selected area diffraction (SAD) pattern are attributed to the pre-martensitic phase. Residual martensite plates are evident in Figure 5c.

Dislocations generated during the transformation facilitate plastic relaxation of the strain energy stored during the forward MT. Because the stored energy provides a mechanical restoring force for the reverse MT, a higher chemical force must drive the reverse MT, causing A_s to increase. Notice in Figure 4 that A_s rises greatly compared to M_s in tension; hence, dislocation generation is dominant in tension. Although the change

of transformation temperatures and temperature hysteresis ΔT_m after aging is asymmetric, the stress hysteresis grows the same amount in tension and compression (Fig. 2 inset). This shows that the influences of dual-phase microstructure depend on a stress state at low stress levels that is achievable only in the $\varepsilon - T$ case.

Precipitation is expected to lower recoverable strain levels because the volume fraction of material undergoing the transformation is reduced due to the γ -phase, and the matrix composition is altered in a similar way to that of NiTi [2]. The fact that large tensile and compressive strains prevail implies that particle sizes and spacing are inhomogeneous because of the short hold time. Importantly, the EDX analysis results show that the nominal composition of the matrix is unchanged, allowing for the realization of strain levels matching the unaged state (Figs. 2 and 3).

In summary, aging NiFeGa alloys in order to introduce γ -phase particles into the microstructure enables the transformation hysteresis to be tailored. Energy dissipation is enhanced because bypassing particles expends frictional work and plastic deformation occurs, though this is not observable macroscopically. Due to these intensified dissipative mechanisms, the hysteresis increases three-fold. Remarkably, the matrix composition is unchanged in the aged alloy and recoverable strains match those observed in the unaged state. The identical strain levels suggest an inhomogeneous distribution of γ -phase within the austenite matrix. Due to the low iso-stresses applied for the $\varepsilon - T$ response, we find a dependence of the influence of aging on stress state. In tension, dislocation generation is intense, producing a much larger increase in thermal hysteresis and transformation temperatures as the iso-stress is elevated.

The work was supported by a grant CMS-0428428, the National Science Foundation, Division of Civil and Mechanical Systems.

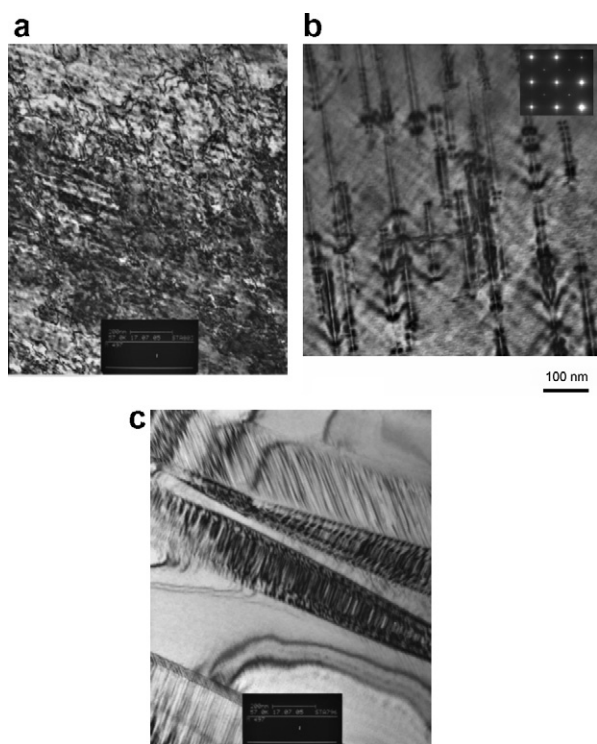


Figure 5. Transmission electron microscopy (TEM) micrographs after thermal cycling in tension showing (a) dense dislocation arrays, (b) dislocations that are likely nucleation centers for the pre-martensitic tweed contrasts creating the streaks in the inset selected area diffraction (SAD) pattern, and (c) residual martensite.

- [1] E. Hornbogen, *Acta Metall.* 33 (1985) 595.
- [2] K. Gall, H. Sehitoglu, Y. Chumlyakov, I.V. Kireeva, *Acta Mater.* 47 (1999) 1203.
- [3] J. Khalil-Allafi, A. Dlouhy, G. Eggeler, *Acta Mater.* 50 (2002) 4255.
- [4] Y. Sutou, N. Kamiya, T. Omori, R. Kainuma, K. Ishida, K. Oikawa, *Appl. Phys. Lett.* 84 (2004) 1275.
- [5] F. Masdeu, J. Pons, C. Seguí, E. Cesari, J. Dutkiewicz, *J. Magn. Magn. Mater.* 290–291 (2005) 816.
- [6] R.F. Hamilton, C. Efstathiou, H. Sehitoglu, Y. Chumlyakov, *Scripta Mater.* 54 (2006) 465.
- [7] R.F. Hamilton, H. Sehitoglu, C. Efstathiou, H.J. Maier, *Acta Mater.*, in press.
- [8] T. Omori, N. Kamiya, Y. Sutou, K. Oikawa, R. Kainuma, K. Ishida, *Mater. Sci. Eng. A* (2004) 403.
- [9] K. Oikawa, T. Ota, T. Omori, Y. Tanaka, H. Morito, A. Fujita, R. Kainuma, K. Fukamichi, K. Ishida, *Appl. Phys. Lett.* 81 (2002) 5201.
- [10] R. Santamarta, J. Font, J. Muntasell, F. Masdeu, J. Pons, E. Cesari, J. Dutkiewicz, *Scripta Mater.* 54 (2006) 1105.
- [11] R.F. Hamilton, H. Sehitoglu, C. Efstathiou, H.J. Maier, Y. Chumlyakov, *Acta Mater.* 54 (2006) 587.